NASA/TM–2013-217796

Global Response of the Space Shuttle External Tank with the Presence of Intertank Stringer Cracks and Radius Blocks

Andrew E. Lovejoy
Langley Research Center, Hampton, Virginia

Charles C. Rankin
Rhombus Consultants Group, Inc., Palo Alto, California

January 2013

NASA STI Program . . . in Profile

Since its founding, NASA has been dedicated to the advancement of aeronautics and space science. The NASA scientific and technical information (STI) program plays a key part in helping NASA maintain this important role.

The NASA STI program operates under the auspices of the Agency Chief Information Officer. It collects, organizes, provides for archiving, and disseminates NASA's STI. The NASA STI program provides access to the NASA Aeronautics and Space Database and its public interface, the NASA Technical Report Server, thus providing one of the largest collections of aeronautical and space science STI in the world. Results are published in both non-NASA channels and by NASA in the NASA STI Report Series, which includes the following report types:

- TECHNICAL PUBLICATION. Reports of completed research or a major significant phase of research that present the results of NASA Programs and include extensive data or theoretical analysis. Includes compilations of significant scientific and technical data and information deemed to be of continuing reference value. NASA counterpart of peer-reviewed formal professional papers, but having less stringent limitations on manuscript length and extent of graphic presentations.

- TECHNICAL MEMORANDUM. Scientific and technical findings that are preliminary or of specialized interest, e.g., quick release reports, working papers, and bibliographies that contain minimal annotation. Does not contain extensive analysis.

- CONTRACTOR REPORT. Scientific and technical findings by NASA-sponsored contractors and grantees.

- CONFERENCE PUBLICATION. Collected papers from scientific and technical conferences, symposia, seminars, or other meetings sponsored or co-sponsored by NASA.

- SPECIAL PUBLICATION. Scientific, technical, or historical information from NASA programs, projects, and missions, often concerned with subjects having substantial public interest.

- TECHNICAL TRANSLATION. English-language translations of foreign scientific and technical material pertinent to NASA's mission.

Specialized services also include organizing and publishing research results, distributing specialized research announcements and feeds, providing information desk and personal search support, and enabling data exchange services.

For more information about the NASA STI program, see the following:

- Access the NASA STI program home page at *http://www.sti.nasa.gov*

- E-mail your question to help@sti.nasa.gov

- Fax your question to the NASA STI Information Desk at 443-757-5803

- Phone the NASA STI Information Desk at 443-757-5802

- Write to:
  STI Information Desk
  NASA Center for AeroSpace Information
  7115 Standard Drive
  Hanover, MD 21076-1320

NASA/TM–2013-217796

Global Response of the Space Shuttle External Tank with the Presence of Intertank Stringer Cracks and Radius Blocks

Andrew E. Lovejoy
Langley Research Center, Hampton, Virginia

Charles C. Rankin
Rhombus Consultants Group, Inc., Palo Alto, California

National Aeronautics and
Space Administration

Langley Research Center
Hampton, Virginia 23681-2199

January 2013

Available from:

NASA Center for AeroSpace Information
7115 Standard Drive
Hanover, MD 21076-1320
443-757-5802

Table of Contents

Table of Contents 1
Introduction 2
Background 2
Finite Element Modeling 2
  Legacy ET-96 model 3
    LOX Tank 3
    Intertank 4
    Loads and Boundary Conditions 4
  Refined ET-137 model 4
    Modified LOX Tank 5
    Modified Intertank 5
    Stringer Cracks and Radius Block Repair 5
    Loads and Boundary Conditions 6
Analysis 6
Results 6
STAGS Capability Improvements 7
  Tabular Input Capability 7
    Loads 7
    Finite Element Property Information 7
    Other Input 8
Conclusions 8
References 9

Introduction

After propellant was loaded into the external tank (ET), the November 5, 2010 launch of Space Shuttle mission STS-133 was scrubbed due to a gaseous hydrogen leak located in a vent line near the ground umbilical and ET connection. Subsequent visual inspections identified cracks in the sprayed-on foam insulation in the forward end of the ET intertank segment, adjacent to the liquid oxygen (LOX) tank, as shown in Figure 1. These cracks necessitated repair of the foam due to debris concerns that violated launch constraints. As part of the repair process, the affected foam was removed to reveal cracks in the underlying external hat stiffeners on the intertank, as shown in Figure 2. Ultimately, five stiffeners were discovered to be cracked adjacent to the LOX tank.

As the managing center for the ET Project, NASA Marshall Space Flight Center (MSFC) coordinated failure investigation and repair activities among multiple organizations, which included the ET prime contractor (Lockheed Martin Space Systems – Michoud Operations), the Space Shuttle Program Office at the NASA Johnson Space Center (JSC), the NASA Kennedy Space Center (KSC), and the NASA Engineering and Safety Center (NESC). STS-133 utilized the external tank designated as ET-137. Many aspects of the investigation have been reported previously in Refs. 1 – 7, which focus on the root cause of the failures, the flight readiness rationale and the local analyses of the stringer failures and repair. This paper summarizes the global analyses that were conducted on ET-137 as part of the NESC effort during the investigation, which was conducted primarily to determine if the repairs that were introduced to the stringers would alter the global response of the ET. In the process of the investigation, a new STAGS tabular input capability was developed to more easily introduce the aerodynamic pressure loads using a method that could easily be extended to incorporate finite element property data such as skin and stiffener thicknesses and beam cross-sectional properties.

Background

The Space Transportation System (STS) consists of the Space Shuttle, the ET and solid rocket boosters (SRBs), as shown in Figure 3. Throughout its lifetime, the design of the external tank has evolved,[8] with the most recent design, referred to as the superlightweight tank (SLWT), being introduced in the late 1990's when the first SLWT designated ET-96 flew. The SLWT, depicted in Figure 4, was developed to reduce the total system weight to facilitate the Space Shuttle reaching a 51.6° high-inclination orbit without having to significantly reduce the weight of the payload. The nonlinear behavior of thin-walled portions of the SLWT was an important design consideration, due to the fact that the LOX tank experiences significant compressive stresses. The nonlinear behavior of the SLWT LOX tank was studied by Nemeth, et al.[9] A legacy model of the ET-96 design developed for use in Ref. 9 was used as the starting point for the current analyses.

Finite Element Modeling

The legacy ET-96 model developed for use in Ref. 9 utilized the STAGS[10] finite element code. Since it was used as the starting point for the current analyses, the ET-96 model is described first to establish the basic, original design of the SWLT. Next, the ET-137 model used for the current analyses is described to identify the changes that have been made to the SWLT over its life. The details of both models are included, in part, to emphasize how the tabular input method that was developed and presented herein can simplify and speed up model generation. The finite element models include a significant number of structural details, including many thickness variations that represent the tailoring used to reduce structural weight. Included with the basic STAGS model input file are numerous user-written subroutines. User-written subroutines are described in the STAGS manual, and are FORTRAN codes that are used to input

nearly any model input required.[10] User routines such as LAME, WALL, CROSS, UPRESS and UTEMP were used to define reference surface geometries, tapered shell walls and stiffener cross sections, and to define complex force, temperature and pressure distributions in the models described herein. The user-written subroutines are independent of the mesh discretization, which simplifies mesh modification, such as for mesh convergence studies or local mesh refinement. Details of the legacy model and the refined ET-137 model are presented below.

Legacy ET-96 model

The legacy ET-96 model consisted of the LOX tank and the intertank, which is an intermediate structure connecting the LOX and LH2 tanks. The intertank includes the SRB beam that connects the SRBs to the forward portion of the ET and passes through the intertank. The legacy model, two meshes of which are shown in Figure 5, consisted of the section of ET from the forward cover plate end of the LOX tank (shown in Figure 6), at XT = 371 in., to the plane formed between the mating surfaces of the intertank (shown in Figure 7) and the liquid hydrogen (LH2) tank flange, located at XT = 1123.15 in. Coordinates XT are referenced to a global coordinate system located forward of the ET, with the XT-axis aligned with the ET axis as shown in Figure 3. The finite element mesh was generated using STAGS shell units. STAGS includes a library of common shell types, including a cylinder, cone, sphere or ellipsoid, that are defined by providing parametric representation data. Additionally, through the LAME user-written subroutine, shell units for shell types not included in the STAGS library can be parametrically generated. The general coarse model is shown in Figure 5a, and a locally refined model is shown in Figure 5b. Locally refined models were used to improve the analysis accuracy within regions of interest by modifying the STAGS shell unit input data.

LOX Tank

The LOX tank components are identified in Figure 6. The SLWT LOX tank is a thin-walled monocoque shell fabricated primarily from 2195 aluminum-lithium alloy. Main structural components of the LOX tank, as identified in Figure 6, are the forward ogive that is fabricated using 8 gore panels, the aft ogive that is fabricated using 12 gore panels, the barrel section that is fabricated using 4 panels, and the aft elliptical dome that is fabricated using 12 gore panels. The total length of the LOX tank from the forward cover plate to the aft dome is approximately 49 ft, with a maximum diameter of approximately 27.5 ft. Additional details are provided in Reference 9.

The LOX tank finite element model made use of several shell unit library shells, such as annular plate, cylinder, cone and ellipsoid, and used the LAME subroutine to define the forward and aft ogive sections of the LOX tank. Thickness variations of the LOX tank segments were included using the WALL user-written subroutine. The forward ogive portion had thicknesses that varied from 0.08 in. to 0.157 in. in both the axial and circumferential directions. In a similar manner, the aft ogive portion had thicknesses that varied from 0.081 in. to 0.190 in., the barrel portion had thicknesses that varied from 0.140 in. to 0.385 in., and the aft dome had thicknesses that varied from 0.088 in. to 0.125 in. The aft dome closeout is a spherical cap segment, with the LOX suction fitting and covered manhole being neglected. Locally thickened regions, such as regions to support external cable trays, were also included in the model. Weld land details were included using discrete rectangular beams that had variable thickness and width. Changes in the cross section along the length of a weld land were implemented using the user-written subroutine CROSS. In a similar manner, circumferential stiffeners on the aft dome were included as discrete beams. Other details included in the model, which are common or unchanging between ET-96 and ET-137, are provided in Ref. 9.

Intertank

The intertank is a right-circular cylinder fabricated from 2090 and 7075 aluminum alloys. Components of the intertank are identified in Figure 7. The intertank begins at the forward flange located at XT=852.8 in. where it connects to the LOX tank y-ring junction, and ends at the aft flange located at XT=1123.15 in. where it connects to the LH2 tank. The main structural components of the intertank are six 45° curved panels with external longitudinal hat stiffeners, two 45° integrally machined thrust panels, internal ring frames, and the SRB beam that connects through the thrust panels. The intertank is approximately 22.5 ft long with a diameter of approximately 27.5 ft.

Skin shell thicknesses in the six hat-stiffened panels range from 0.067 to 0.221 in., which includes the skin only regions and the regions where doublers are included with the skin. Hat stiffener thicknesses range from 0.043 to 0.063 in., they are 2.5 in. deep, and they taper from a width of 2.57 in. at the skin to 1.38 in. at the top. Hat stiffener spacing is 7.2 in. The hat-stiffened panels were modeled as orthotropic shells using a smeared stiffener approach that was incorporated through the WALL and CROSS user-written subroutines. The thrust panels are integrally machined with blade stiffeners. Thrust panel skin thicknesses ranged from 0.090 to 2.062 in., and stiffener thicknesses ranged from 0.180 to 1.050 in. An equivalent orthotropic shell with variable thickness was used to model the thrust panel, and similar to the hat-stiffened panels, the properties were incorporated using the WALL and CROSS subroutines. The internal ring frames were included as discrete beams, as was the SRB beam. Again, additional details that are unchanging between ET-96 and ET-137 are provided in Ref. 9.

Loads and Boundary Conditions

Loads on the portion of the ET that was modeled include interface loads at the mating plane between the intertank and LH2 tank (XT = 1123.15 in.), ullage and LOX pressures, aerodynamic loads, a temperature profile, structural weight and additional nonstructural weight (such as the slosh baffles), and SRB interface loads. These loads are identified in Figure 8. For this model, the SRB loads were replaced by restraints to eliminate rigid body motion, and the developed reaction forces could be checked to ensure equilibrium was satisfied. The interface loads at the mating plane between the intertank and LH2 tank were assigned to a load set that was considered to be the active loads, which would give rise to destabilizing stresses. The remaining loads, which include internal and aerodynamic pressures and temperatures, were assigned to a second load set that was unchanging, and were considered to be the passive loads acting on the model.

The interface loads at the mating plane between the intertank and LH2 tank were defined using the STAGS least squares loading and moving plane boundary feature. The least squares loading converted the concentrated forces and moments provided at the mating plane into statically equivalent shell wall stress resultants, and the moving plane boundary enforced the geometric requirement that all nodes within the plane remain coplanar during deformation. LOX pressure was defined in the UPRESS user-written subroutine, and the temperature distribution was defined in the UTEMP user-written subroutine. Aerodynamic loading on the outside of the ET is considerably more complex, and pressure data was converted into a Fourier series representation for the pressure field that could be defined in the UPRESS subroutine. Nonstructural weight was defined as uniformly distributed line loads at the appropriate locations.

Refined ET-137 model

Many modifications to the legacy ET-96 model were required to accurately represent the ET-137 tank.

Modifications were necessary to incorporate the many design changes in the ET between ET-96 and ET-137, to account for cracked stringers, and to incorporate the radius block repair. The radius block repair is a local reinforcement of the external stringers where they terminate and attach to the intertank panels. Details of the radius block repair are provided in Ref. 1.

The mesh used for the ET-137 stringer crack study is shown in Figure 9. Note the significant overall refinement of the mesh compared to the baseline legacy ET-96 model shown in Figure 5. This refinement was incorporated for several reasons. First, as reported in Ref. 9, increasing the mesh density increases the likelihood the beams representing the weld lands and stiffeners are closer to their actual locations, since in creating the model, beams were moved to node closest to the actual location of a weld land or stiffener. Also, in anticipation of including the radius block repair, the mesh in the intertank was required to be sufficiently refined to accurately locate the radius blocks at the intertank stiffener locations. Additionally, at the time the legacy model was developed and used, local mesh refinement was incorporated to provide more accurate predictions, while keeping the number of degrees of freedom as small as possible. However, the significant increase in degrees of freedom introduced by the overall mesh refinement for ET-137 was not detrimental to solution time when compared to the legacy model analyses. This is due to the increase in computer speed, and the introduction of a new sparse solver in STAGS since the legacy model was developed and analyzed. Details of other model changes for ET-137 are summarized below for the LOX tank and intertank.

Modified LOX Tank

Multiple modifications to the LOX tank occurred to the ET between ET-96 and ET-137. Some of the 2195 aluminum-lithium alloy was replaced by 2219 aluminum alloy. As a result of the material change, numerous thickness changes were required in the forward ogive, aft ogive and aft dome. Modified thicknesses for the forward ogive ranged from 0.085 inches to 0.140 inches, for the aft ogive ranged from 0.096 inches to 0.190 inches, and for the aft dome ranged from 0.111 inches to 0.186 inches. In addition, the number of circumferential stiffeners and their thicknesses were changed. To implement these modifications, changes to the WALL subroutine were required.

Modified Intertank

Modifications to the intertank between ET-96 and ET-137 were limited to the thrust panels. The thrust panel material was changed from 2219 aluminum alloy to 2297 aluminum-lithium alloy. Skin thicknesses in the thrust panels ranged from 0.090 inches to 2.062 inches, the same as in ET-96, but the skin thickness mapping changed. The new thrust panel stiffener thicknesses ranged from 0.170 inches to 1.050 inches. To implement these modifications required significant changes to the WALL and CROSS subroutines.

Stringer Cracks and Radius Block Repair

To approximate the cracked stringers in the model, the thickness of the stringer was set to zero for the length of the crack. The cracks were included in the model by modifying the WALL subroutine. The radius blocks were included as additional beam elements located at the ends of the stringers. As previously mentioned, the mesh refinement was partially driven by the desire to ensure that the radius block elements were place at the proper locations, both axially and circumferentially. The radius blocks were fabricated from 2024 aluminum alloy.

Loads and Boundary Conditions

Loads and boundary conditions for the ET-137 were modeled in the same way as for the legacy model, with the exception of the pressure loads that were introduced using the method described in the appendix. The STAGS tabular implementation described in the appendix greatly simplifies the process for introducing the pressure loads, and eliminates the need for the UPRESS user-written subroutine.

Analysis

The developed ET-137 finite element model was used to examine the global response for several load cases. Linear static and linear bifurcation analyses were conducted. Stress resultants, i.e. running loads, and the buckling loads and modes were compared between a baseline pristine model, a model with cracked stringers, and a model with radius block fixes included. The load cases examined and the results are now presented.

Three load cases were examined. The first load case (LC1) is a prelaunch load case that is identical to one of the prelaunch load cases of Ref. 9. This load case corresponds to full LH2 and LOX tanks, but does not include the ullage pressure. The second (LC2) and third (LC3) load cases were ones that were determined to be critical for the ET-137 tank. Case LC2 is a high-q (high dynamic pressure) ascent case at Mach 1.8, and case LC3 is a high-q ascent case at Mach 2.2. Load case data for LC2 and LC3 were provided to the NESC team by the Space Shuttle contractor.

Results

Analyses of ET-137 with the stringer cracks indicated no significant detrimental global responses compared to the pristine tank. Since ET-137 was not expected to fly without the radius block repairs to the intertank external stringers, the results presented herein focus on the analyses of the repaired ET-137.

The axial running load, Nx, was compared between the pristine and radius-block-repaired model to determine if inclusion of the radius blocks influenced the load distribution. Figure 10 shows the LC1 linear analysis Nx comparison for the (a) pristine and (b) radius block repaired ET-137. No significant variation in the Nx values is seen. Similar agreement was seen for LC2 and LC3, indicating that the presence of the radius blocks does not influence the load distribution in ET-137. This is not surprising because the radius blocks were included on all of the stringers, resulting is a reasonably uniform increase of local stiffness around the circumference.

While it was not unexpected for the radius blocks to have little influence on the running load, there remained a distinct possibility that the radius blocks could influence the buckling loads and modes because of the local increase in bending stiffness. The load case LC1 critical buckling mode for the pristine ET-137 tank is shown in Figure 11, where two views are given to better display the mode shape. The buckling mode shown in Figure 11 is representative of the modes for all three load cases, where all of the critical buckling modes are located in the aft ogive portion of the LOX tank, with the circumferential location being determined by the load case. A similar buckling mode was seen in the radius-block-repaired model. The buckling load factors for both models are compared in Table 1 for all three load cases. Load factors for the radius-block-repaired model were nearly identical to the load factors for the pristine model. Therefore, the buckling response of ET-137 is not degraded by the presence of the radius blocks, and their presence did not change the locations of the critical modes.

STAGS Capability Improvements

With four types of loading, introduction of load for models such as the ET-137 tank is a complex process. Recall that the four types of loading considered in this study are:

1) Acceleration loads of the fluid and other masses not included in the model, accounting for the tilt (attitude) of the vehicle.

2) Ullage pressure.

3) External aerodynamic pressure loading.

4) Reactions due to lumped mass items and structure not modeled with finite elements.

As discussed previously, for the legacy model analyses, the complex aerodynamic pressure distribution was input as a Fourier series representation in the UPRESS subroutine. However, this method necessitates determining an appropriate Fourier series expansion. Since the aerodynamic pressure data can be supplied as a set of tabular data, it was determined that using the tabular data directly was a more efficient method of applying the aerodynamic pressure for determining the resulting nodal loads. The method of utilizing the tabular data in STAGS, the tabular input capability, and other input improvements for ullage and fluid pressure and lumped mass are discussed subsequently.

Tabular Input Capability

Loads

The external aerodynamic loads are interpolated directly from a set of pressure data that is provided in tabular format. The task is made much easier by the fact that each table contains the data value with its associated position coordinates along the global axial model direction (X) and the the angle around the circumference (θ). These coordinates form a rectangular "grid," with each "node" in the grid defining a position in the two orthogonal directions. The coordinate X values are provided, followed by the θ values, followed by the sets of pressure given for each "node." Pressure data sets are given for each fixed X value and span the θ values. The procedure for determining the aerodynamic load at a node in the finite element model, whose location is designated as (X_n,θ_n), is as follows:

1) Use a simple binary search to find the two bracketing coordinates in the X direction such that $X_i \leq X_n \leq X_{i+1}$, where X_i and X_{i+1} are tabular data coordinates. This binary search is extremely efficient, which will permit the use of a large number of positions, as may be necessary in regions of high pressure gradients or for the element property information described below.

2) Do exactly the same as 1) for the θ_n coordinate.

3) Given the pressures at the 4 neighboring points, use the shape functions for a basic 4-node quadrilateral to obtain an interpolated pressure, and exclude values outside the valid range (note, that event never happened in these analyses).

This work involved code modifications to set up a call to a STAGS library routine that does each of these actions.

Finite Element Property Information

Prior to, and during, the tabular method being developed to simplify load introduction to the finite element model, the finite element property information, such as skin and stiffener thicknesses and beam

cross-sectional properties, was incorporated into the model. As with the legacy model, this involved significant FORTRAN programming of user-written subroutines, which included cross section data in the CROSS subroutine, and skin wall data in the WALL subroutine. Relatively minor changes were made to CROSS, some of which had to be made to reflect substantial improvements to the STAGS code. Subroutine WALL was a different matter entirely, where the authors had to verify the rather complicated logic statements that were used to bracket the position for each Gauss point, and which then provided fabrication data (such as skin and stiffener thicknesses) accordingly. The authors believe the substantial work required in generating models like these in the future would be saved if there were access to a "fabrication map" in much the same form as the aerodynamic pressure tables mentioned in the previous section. To implement the data retrieval in STAGS would be even simpler than for the pressure, because after finding the bracketing coordinates using the binary search, it is simply a matter of taking data directly from the table and not interpolating. Each patch would be identified by the coordinates of the node of the resulting "quadrilateral" that has the smallest coordinate values, a procedure exactly the same as locating an element in a shell unit by providing the row and column indices that are the smallest for a given element. This procedure has actually been tested on an unrelated problem and found to be extremely efficient. Most of the labor is then concentrated in forming the input fabrication table, which once established, is very easy to modify. However, in order to program the subroutines, the geometric data, such as the skin and stiffener thicknesses, has to be compiled. Since this is typically accomplished by developing a map of the geometric quantity, developing the tabular data of the geometric quantity becomes rather trivial.

Other Input

Ullage and fluid pressure loading are readily handled by the method of Ref. 9. However, the current approach incorporates the simplification that both the fill level and ullage pressure have been converted to parameters given in the STAGS input deck. Additionally, the tilt angle is obtained from the acceleration vector, which is also provided in the STAGS input deck. The user-written subroutine UPRESS was revised to include as much parameterization as possible to achieve rapid model adjustments at a minimum of effort.

Finally, to generate the reactions caused by lumped masses and other structures not included in the model, a script was created that takes model input data and the acceleration vector for the current load case, and outputs the relevant quantities needed to account for these masses, which included data for both line and point loads. This procedure was essential to reduce hand-input errors and to save labor. The authors believe that the labor saved by implementing the above capability improvements was a substantial percentage of the total work involved.

Conclusions

In order to investigate the effect of the cracked intertank stringers, and the radius block repairs, a legacy ET-96 tank finite element model was updated to represent the ET-137 tank. The finite element model included the LOX tank and the intertank, and was considered sufficient to investigate the presence of the cracked stringers and radius block repairs that were located at the junction of the LOX tank and intertank. Analyses for three load cases, of which two were flight load cases determined to be critical for the ET-137 tank, were conducted. These analyses indicated that the presence of the cracks and radius block repairs do not significantly influence the global response of the ET-137 tank. Additionally, the expanded capabilities that were developed and implemented in STAGS greatly simplified the modeling and analysis process, reducing the time required to perform the assessment.

Acknowledgements

The authors would like to thank the NESC and Drs. Ivatory S. Raju and Kenny B. Elliot for their support of this work.

References

[1]Wingate, R., "Stress Analysis and Testing at the Marshall Space Flight Center to Study Cause and Corrective Action of Space Shuttle External Tank Stringer Failures," Paper AIAA-2012-1776, 53rd AIAA/ASME/ASCE/AHS/ASC Structures, Structural Dynamics, and Materials Conference, Honolulu, HI, 23-26 April 2012.

[2]Steeve, B., "STS-133 Space Shuttle External Tank Intertank Stringer Crack Investigation Stress Analysis," Paper AIAA-2012-1777, 53rd AIAA/ASME/ASCE/AHS/ASC Structures, Structural Dynamics, and Materials Conference, Honolulu, HI, 23-26 April 2012.

[3]Knight, N., Song, K., Elliott, K., Raju, I and Warren, J., "Elastic-Plastic Nonlinear Response of a Space Shuttle External Tank Stringer: Stringer-Feet Imperfections and Assembly," Paper AIAA-2012-1778, 53rd AIAA/ASME/ASCE/AHS/ASC Structures, Structural Dynamics, and Materials Conference, Honolulu, HI, 23-26 April 2012.

[4]Knight, N., Warren, J., Elliott, K., Song, K., and Raju, I., " Elastic-Plastic Nonlinear Response of a Space Shuttle External Tank Stringer: Thermal and Mechanical Loadings," Paper AIAA-2012-1779, 53rd AIAA/ASME/ASCE/AHS/ASC Structures, Structural Dynamics, and Materials Conference, Honolulu, HI, 23-26 April 2012.

[5]Oliver, S., "STS-133/ET-137 Tanking Test Photogrammetry Assessment," Paper AIAA-2012-1780, 53rd AIAA/ASME/ASCE/AHS/ASC Structures, Structural Dynamics, and Materials Conference, Honolulu, HI, 23-26 April 2012.

[6]Saxon, J., Wingate, R., Swanson, G., Ondocsin, W. and Boles, T., "Stringer Bending Test Helps Diagnose and Prevent Cracks in the Space Shuttle's External Tank," Paper AIAA-2012-1781, 53rd AIAA/ASME/ASCE/AHS/ASC Structures, Structural Dynamics, and Materials Conference, Honolulu, HI, 23-26 April 2012.

[7]Phillips, D., Saxon, J., and Wingate, R., "Test-Analysis Correlation of the Single Stringer Bending Tests for the Space Shuttle ET-137 Intertank Stringer Crack Investigation," Paper AIAA-2012-1782, 53rd AIAA/ASME/ASCE/AHS/ASC Structures, Structural Dynamics, and Materials Conference, Honolulu, HI, 23-26 April 2012.

[8]http://www.lockheedmartin.com/us/news/press-releases
/2010/september/LockheedMartinEndsExterna.html

[9]Nemeth, M. P., Britt, V. O., Collins, T. J., and Starnes, J. H., Jr., "Nonlinear Analysis of the Space Shuttle Superlightweight External Fuel Tank," NASA TP 3616, December 1996.

[10]Rankin, C. C., Loden, W. A., Brogan, F. A., and Cabiness, H. D., "STAGS Users Manual," Rhombus Consultants Group, Inc., Ste. D201, 1121 San Antonio Rd., Palo Alto, CA 94303, January, 2007.

Table 1: Comparison of ET-137 critical buckling load factors.

Load Case	Pristine	Radius Block Repaired
LC1	3.3611	3.3613
LC2	1.3184	1.3185
LC3	2.1498	2.1501

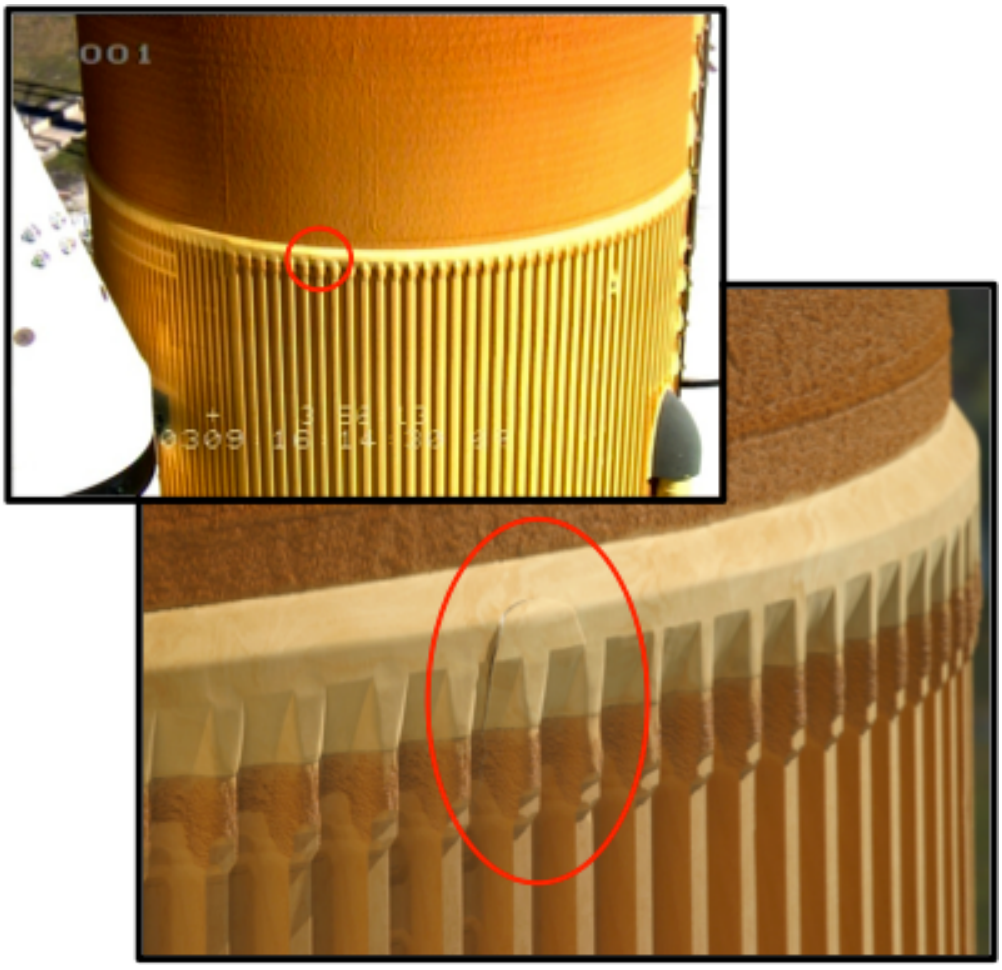

Figure 1: Crack in the ET-127 insulation after tanking. (from Ref. 1)

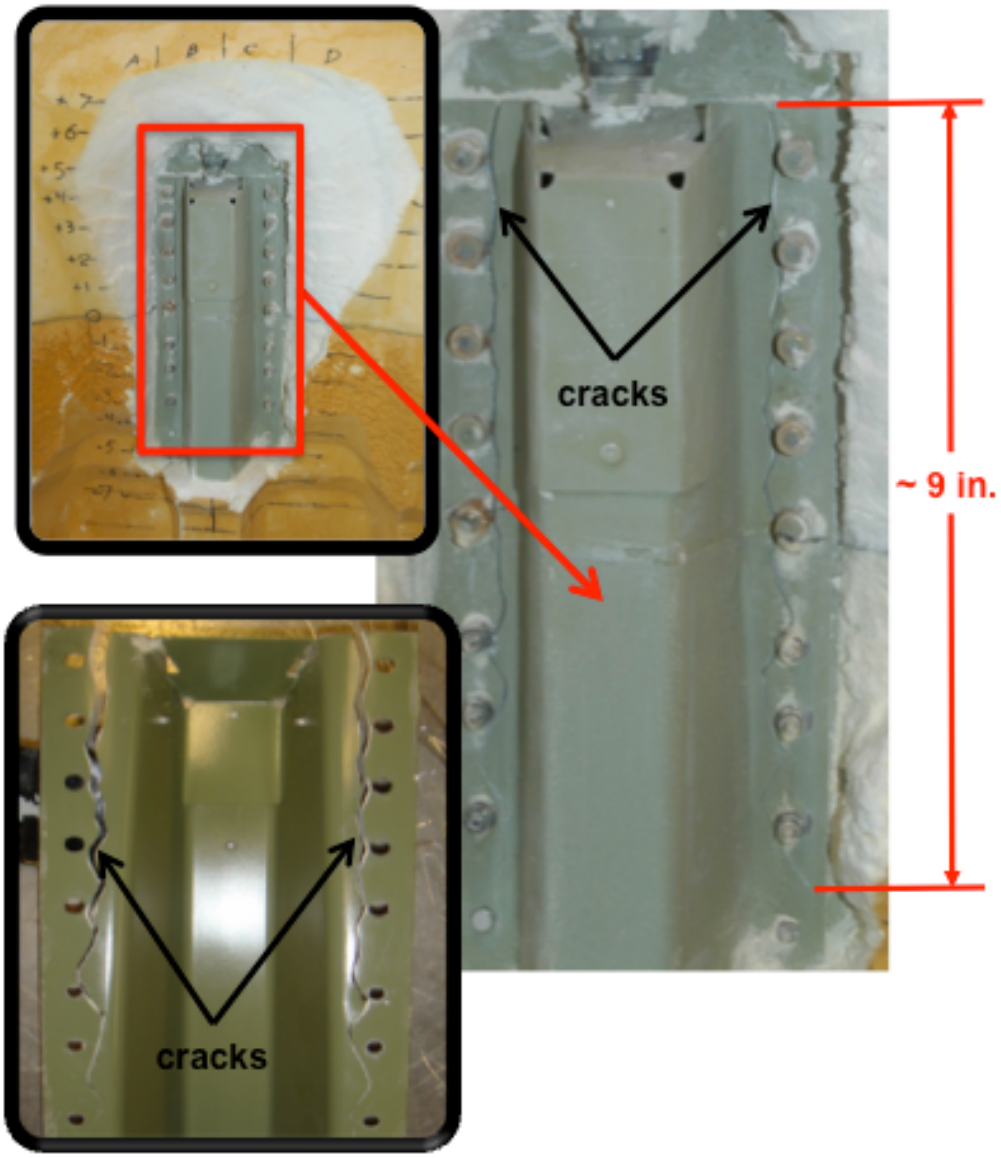

Figure 2: Representative cracks in stringer S7-2. Bottom left inset is stringer S7-2 after removal from ET-137 and with foam residue cleaned off. (adapted from Ref. 1)

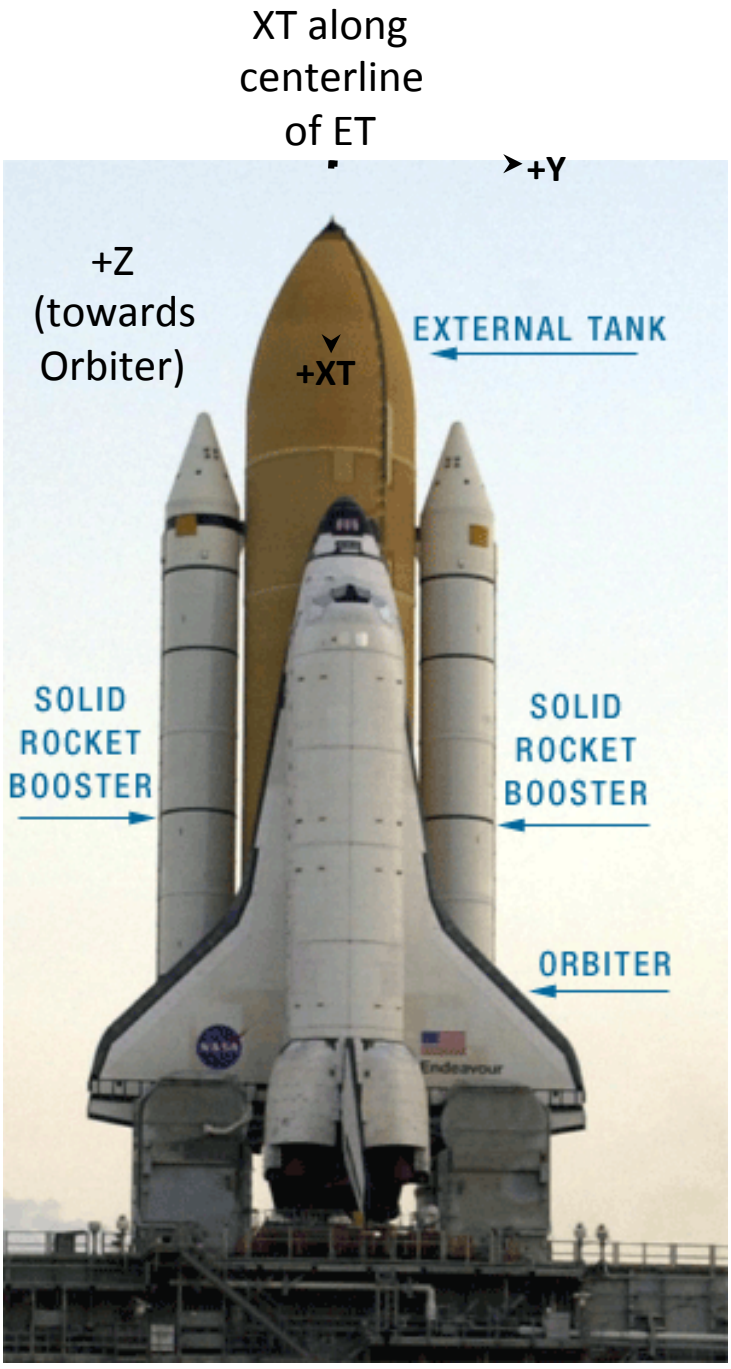

Figure 3: STS components and reference coordinate system.

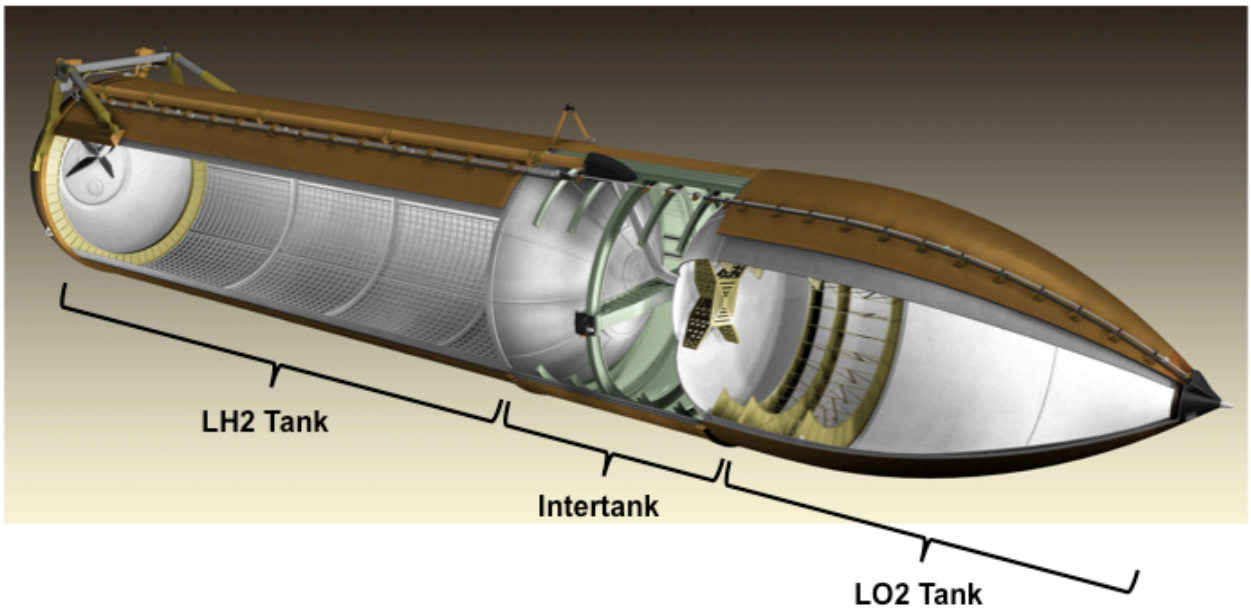

Figure 4: Superlightweight Tank.

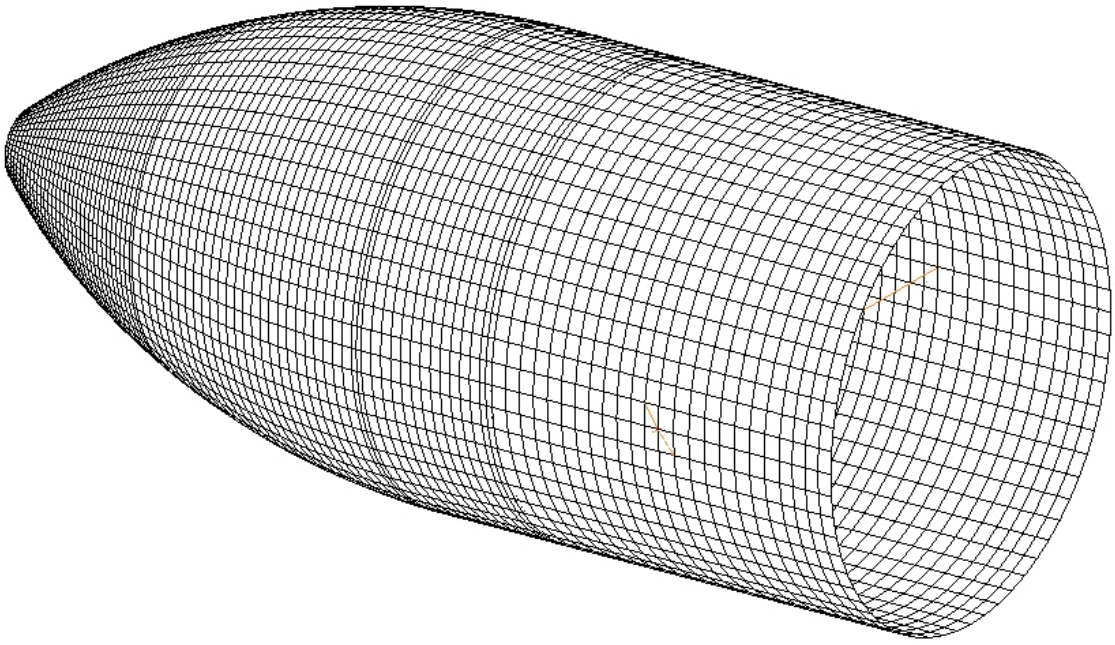

a) coarse

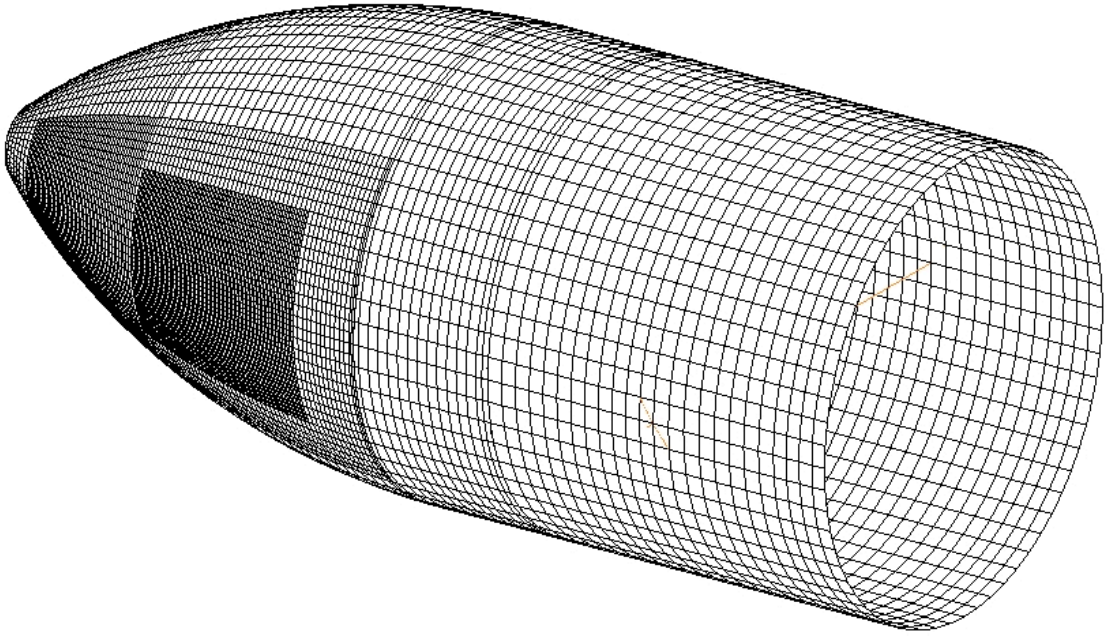

b) locally refined

Figure 5: Legacy ET-96 finite element models.

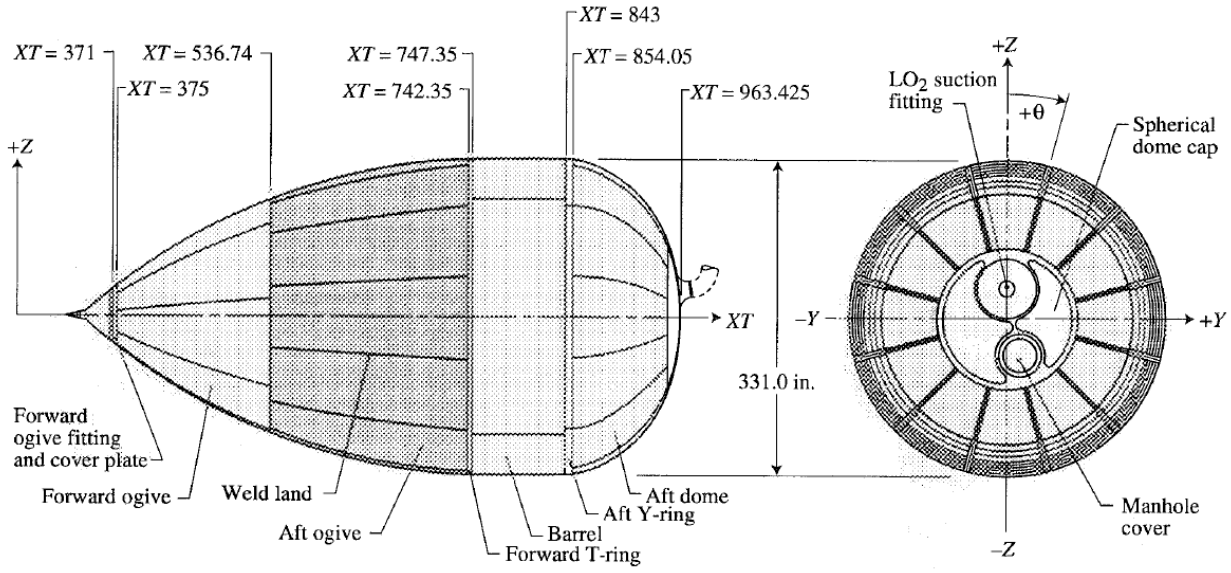

Figure 6. LOX tank structural components. XT values are in inches. (from Ref. 9)

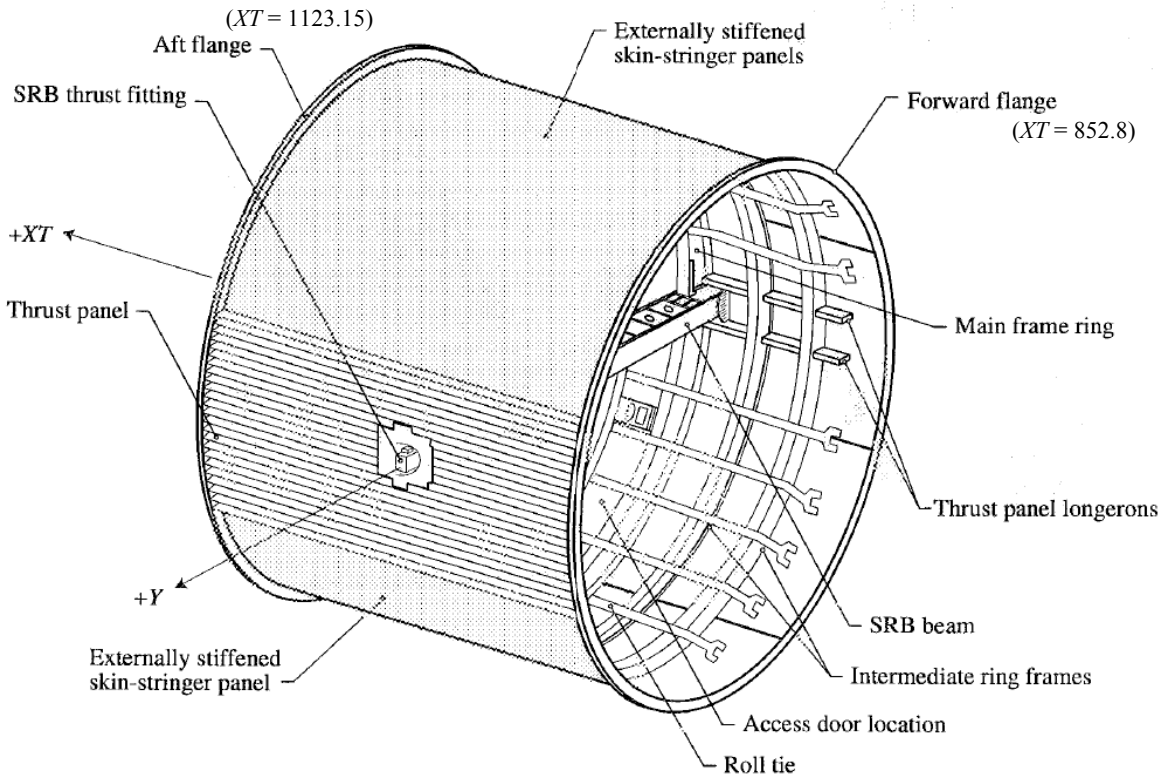

Figure 7: Intertank structural components. (adapted from Ref. 9)

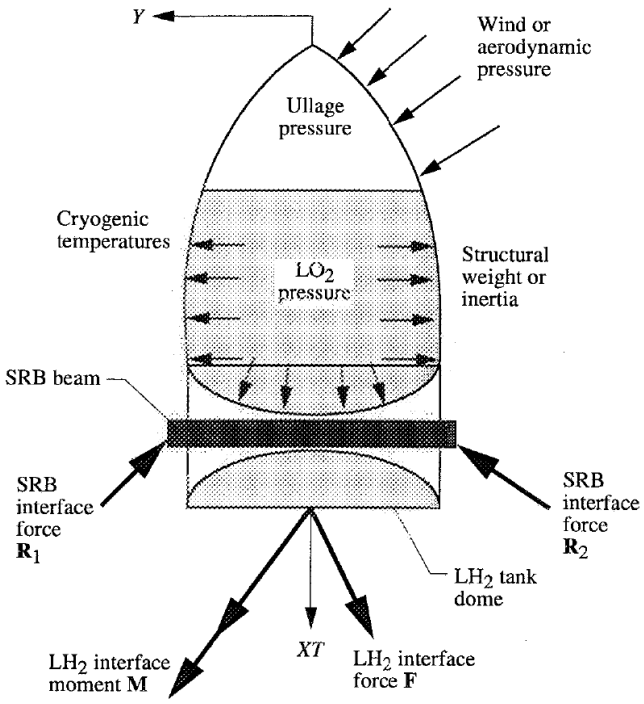

Figure 8: Loads identification. (from Ref. 9)

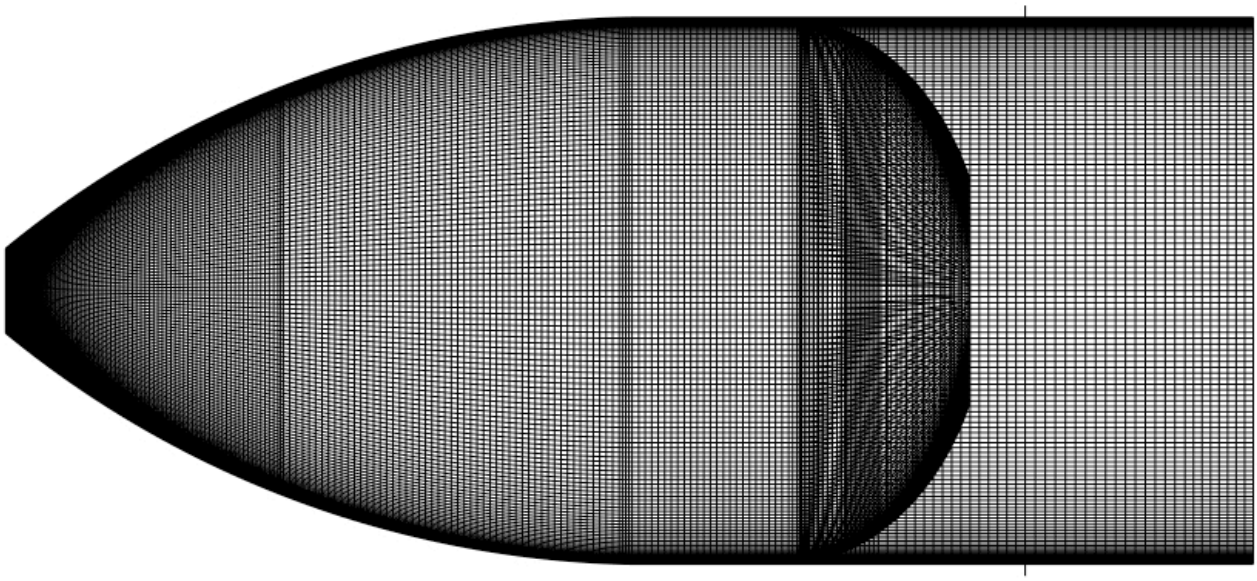

Figure 9: Finite element mesh for ET-137 crack investigation.

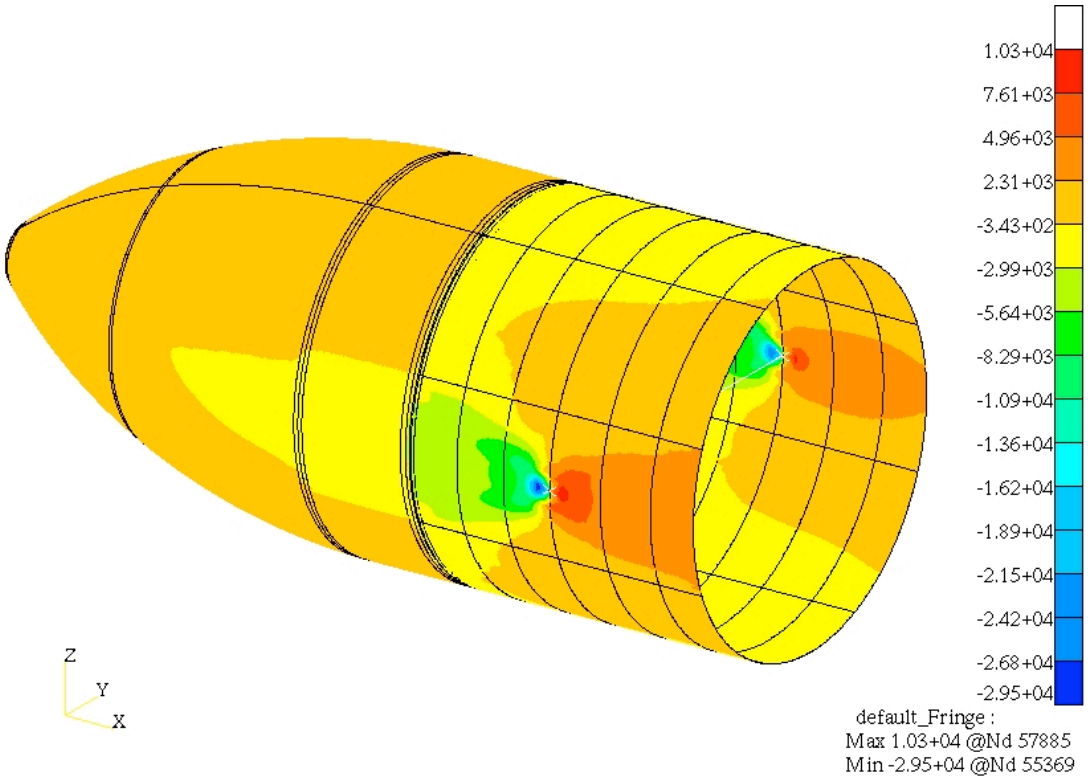

a) Pristine

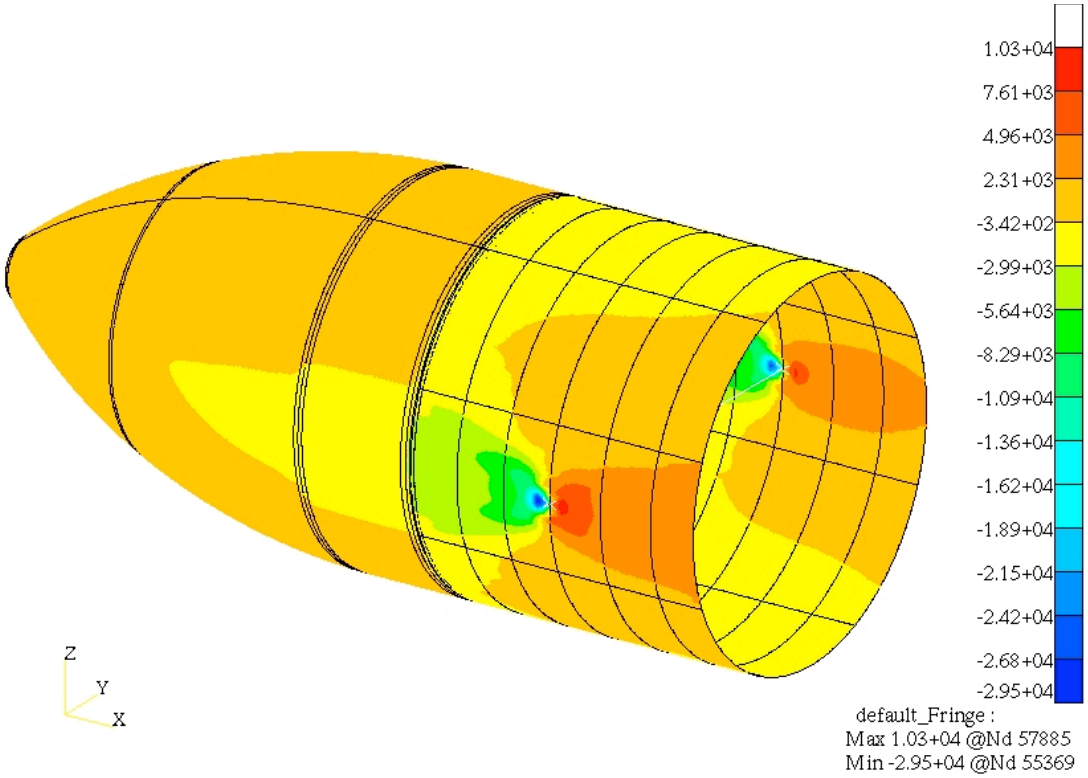

b) Radius block repaired

Figure 10: Comparison of axial running load Nx (lb./in.) for ET-137 tank.

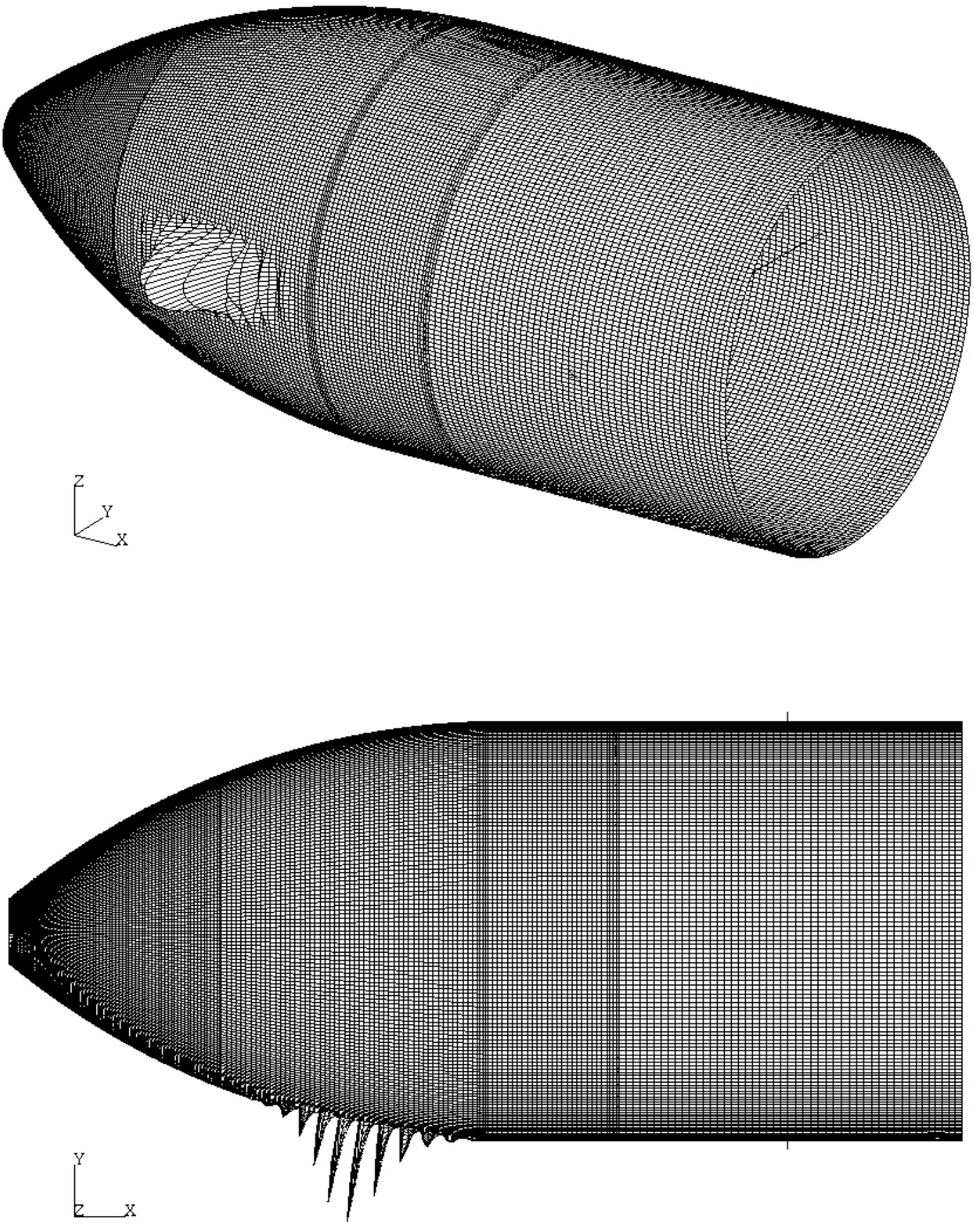

Figure 11: Critical buckling mode for pristine ET-137 subjected to LC1.

REPORT DOCUMENTATION PAGE

Form Approved
OMB No. 0704-0188

1. REPORT DATE *(DD-MM-YYYY)*	2. REPORT TYPE	3. DATES COVERED *(From - To)*
01-01-2013	Technical Memorandum	

4. TITLE AND SUBTITLE

Global Response of the Space Shuttle External Tank With the Presence of Intertank Stringer Cracks and Radius Blocks

5a. CONTRACT NUMBER

5b. GRANT NUMBER

5c. PROGRAM ELEMENT NUMBER

6. AUTHOR(S)

Lovejoy, Andrew E.; Rankin, Charles C.

5d. PROJECT NUMBER

5e. TASK NUMBER

5f. WORK UNIT NUMBER

869021.05.07.09.11

7. PERFORMING ORGANIZATION NAME(S) AND ADDRESS(ES)

NASA Langley Research Center
Hampton, VA 23681-2199

8. PERFORMING ORGANIZATION REPORT NUMBER

L-20215

9. SPONSORING/MONITORING AGENCY NAME(S) AND ADDRESS(ES)

National Aeronautics and Space Administration
Washington, DC 20546-0001

10. SPONSOR/MONITOR'S ACRONYM(S)

NASA

11. SPONSOR/MONITOR'S REPORT NUMBER(S)

NASA/TM-2013-217796

12. DISTRIBUTION/AVAILABILITY STATEMENT

Unclassified - Unlimited
Subject Category 39
Availability: NASA CASI (443) 757-5802

13. SUPPLEMENTARY NOTES

14. ABSTRACT

As part of the NASA Engineering and Safety Center (NESC) assessment of the Space Shuttle External Tank (ET) prior to the STS-133 mission, finite element analyses were performed to determine the response in the region of the liquid oxygen (LOX) tank and intertank. The study was necessitated by cracks in the intertank stringer feet that were discovered after tanking with cryogenic liquid fuel. The global analysis and assessment examined the response of the LOX tank and intertank with the presence of the stringer cracks, and with radius block fixes applied. A legacy Structural Analysis of General Shells (STAGS) finite element model of the ET was updated to reflect LOX tank and intertank design changes. User-written subroutines and STAGS code modifications were used to perform model changes and load application. The STAGS code modification more efficiently and accurately introduced pressure loads to the structure by interpolating tabular pressure data and directly applying loads at the integration points. Analyses of the STS-133 ET were conducted for several prelaunch and flight load conditions. The analyses indicated that the presence of the cracks and radius blocks had negligible effect on the load path and buckling response of the LOX tank and intertank.

15. SUBJECT TERMS

External Tank; STAGS; Space Shuttle

16. SECURITY CLASSIFICATION OF:			17. LIMITATION OF ABSTRACT	18. NUMBER OF PAGES	19a. NAME OF RESPONSIBLE PERSON
a. REPORT	b. ABSTRACT	c. THIS PAGE			STI Help Desk (email: help@sti.nasa.gov)
					19b. TELEPHONE NUMBER *(Include area code)*
U	U	U	UU	23	(443) 757-5802